Contents of this file

Introduction

Fig. S1 shows the AGE and Hammering signal waveform. Fig. S2 Presents the difference of AGEs. Fig. S3 we show how to measure the seismic velocity with hammering signal. Fig. S4 presents the record section of two LFEs. Fig. S5 presents the interevent time distribution. Fig. S6 shows the spectrogram around AGE for DAS and reference station. Fig. S7 is the statistical result of LFEs. Fig. S8 is the icequakes detection with PhaseNet (Zhu & Beroza, 2019). Fig. S9 shows the dispersion curves of FGW with DAS records of inner and outer circles. Fig. S10 shows the dispersion curves of FGW of hammering signal. Fig. S11 shows the number of icequakes and LFEs before and after the AGE. Fig. S12 is the performance of YOLO model. Fig. S13 is the location results for hammering.
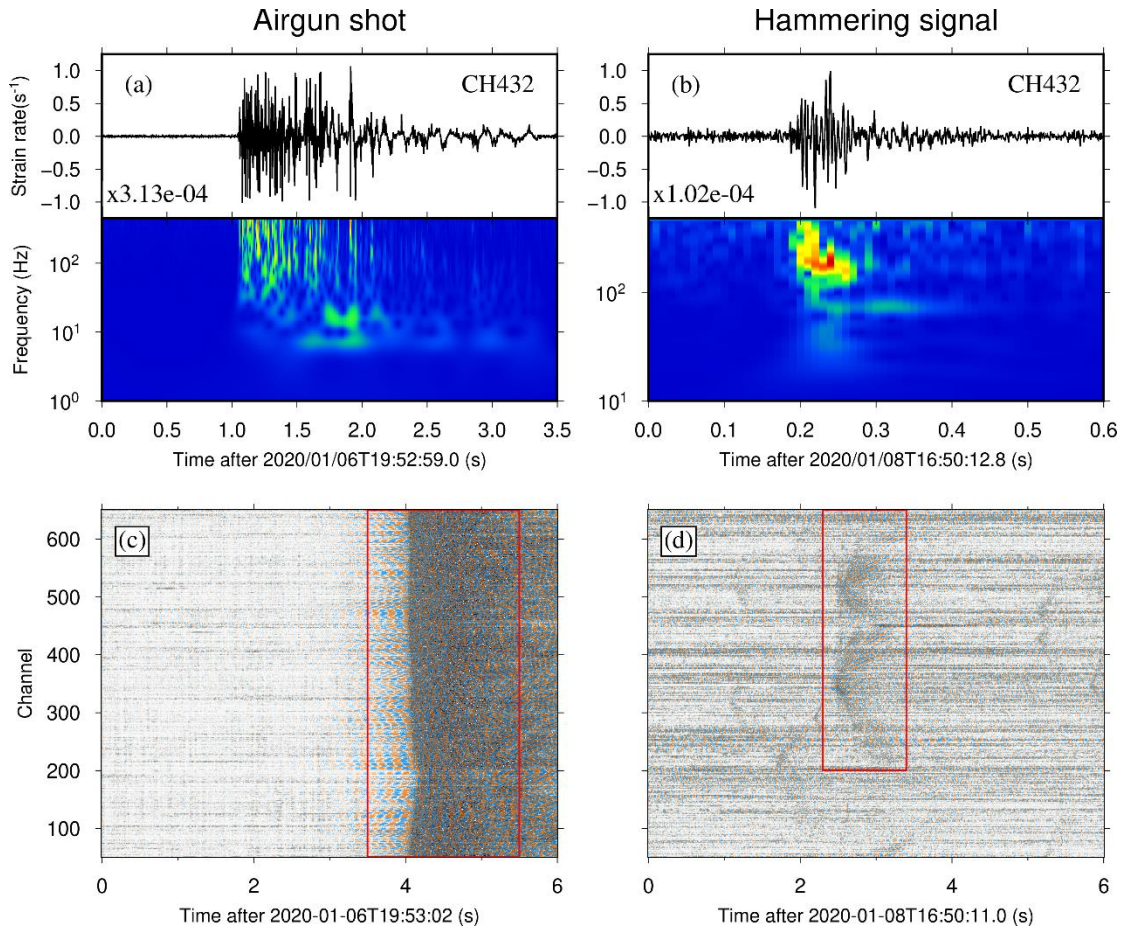
Figure S1. Typical AGE and hammering signal and their spectrogram (a, b) and their record sections (c, d). The signals are marked with red rectangles.
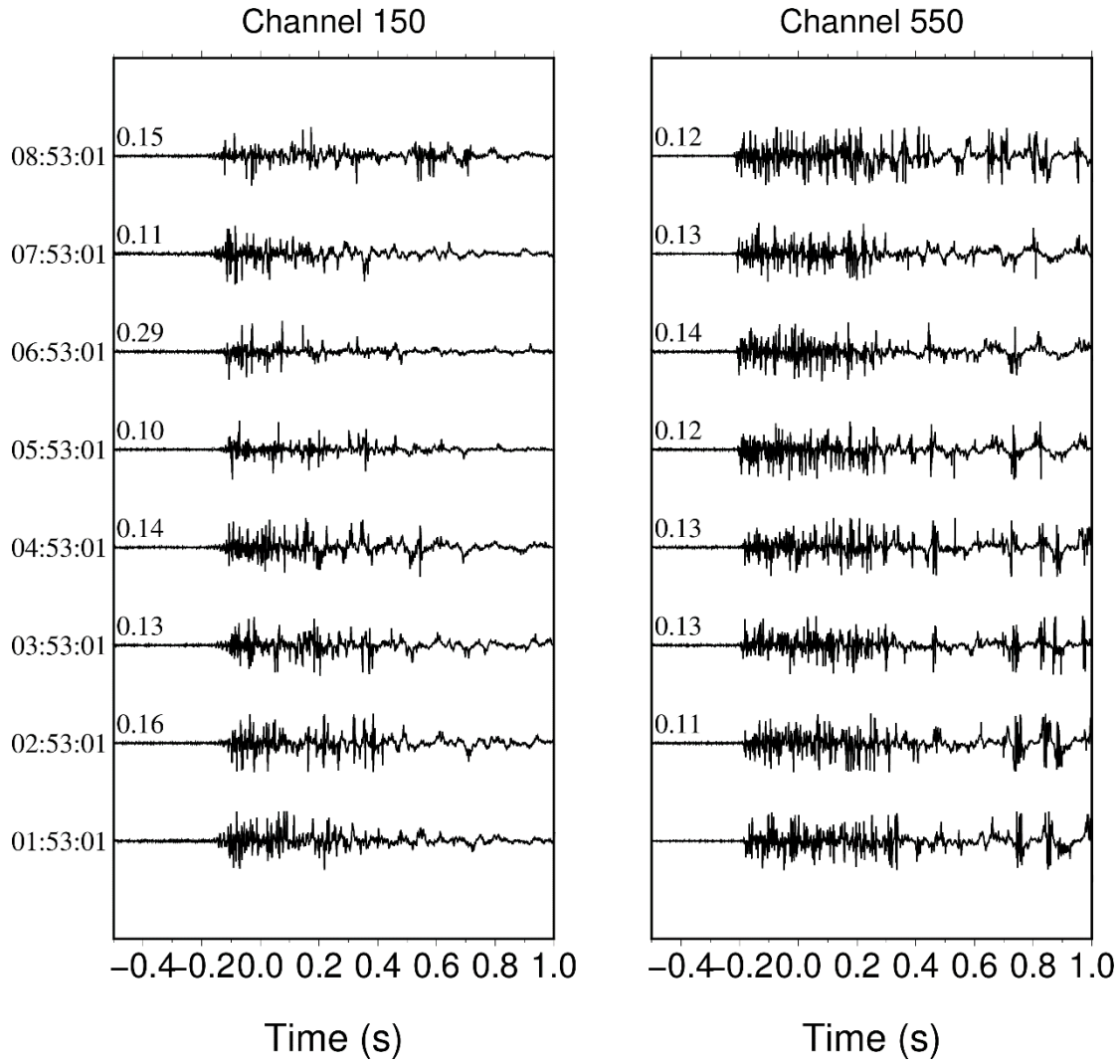
Figure S2. Waveforms of eight DAS AGEs for channel 150 (left) and channel 550 (right). Cross-correlation coefficients between each waveform with the first one at the bottom are shown on the left side of each waveform.
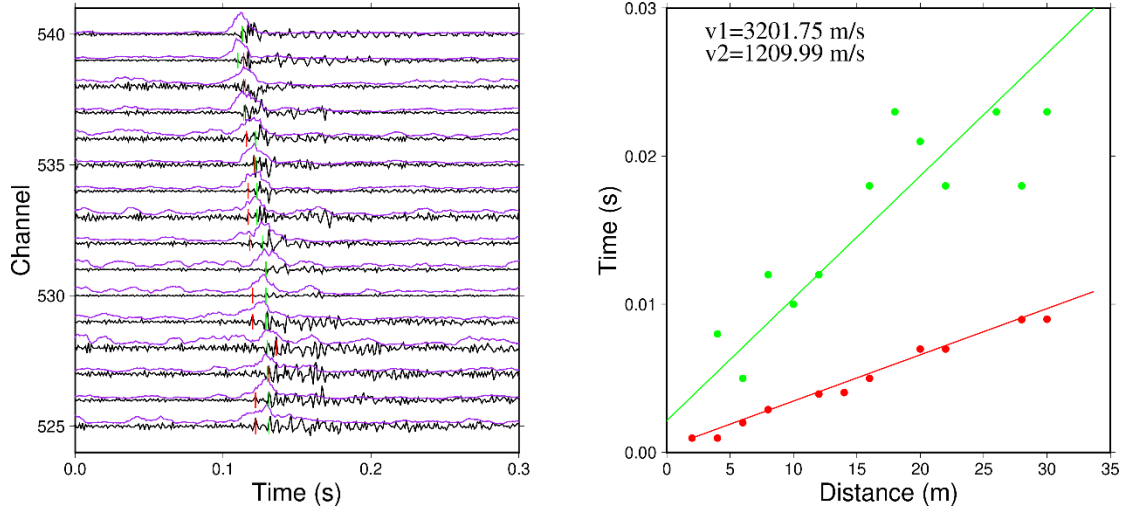
Figure S3. Velocity measurement with hammering signal. Left: Waveform of hammering event (black curves), STA/LTA waveform (purple). The red lines are arrivals by handpick and the green lines are by STA/LTA. Right: corresponding velocity fit.
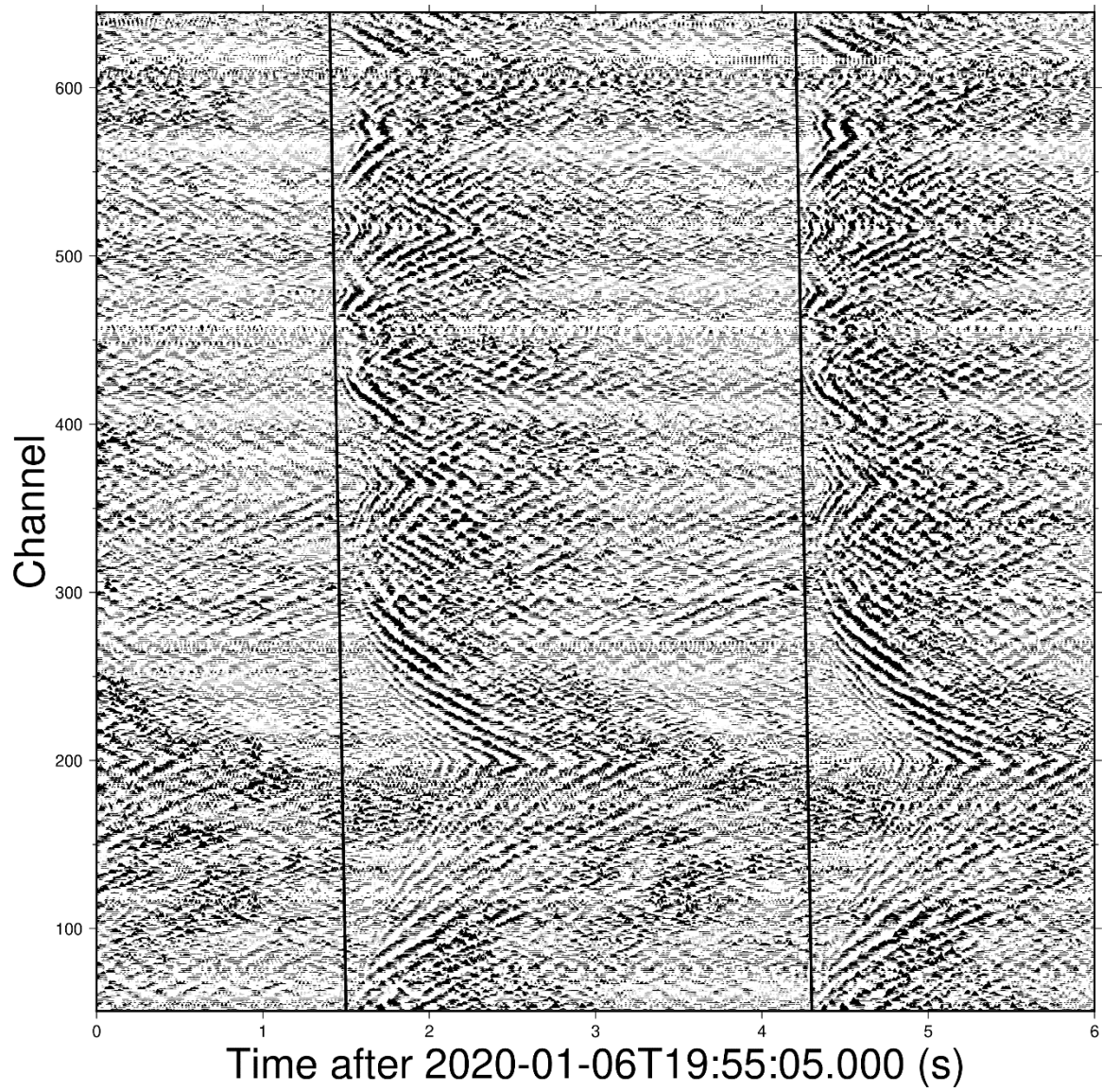
Figure S4. Record section of two close LFEs. Waveforms are bandpass filtered in the frequency band 5-50 Hz. The black straight lines indicate the arrival of the waveforms.
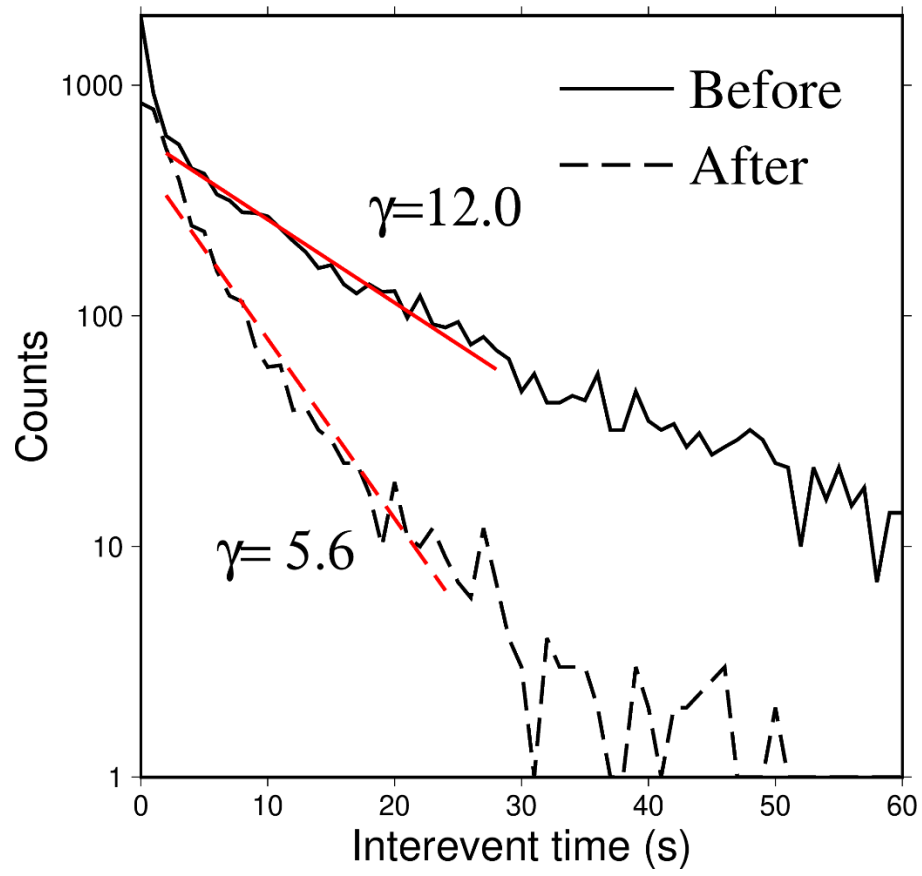
Figure S5. Interevent time distribution of icequakes before (black line) and after (dashed line) the noon of Jan. 9th. Red lines are corresponding fitting results with Poisson distribution.
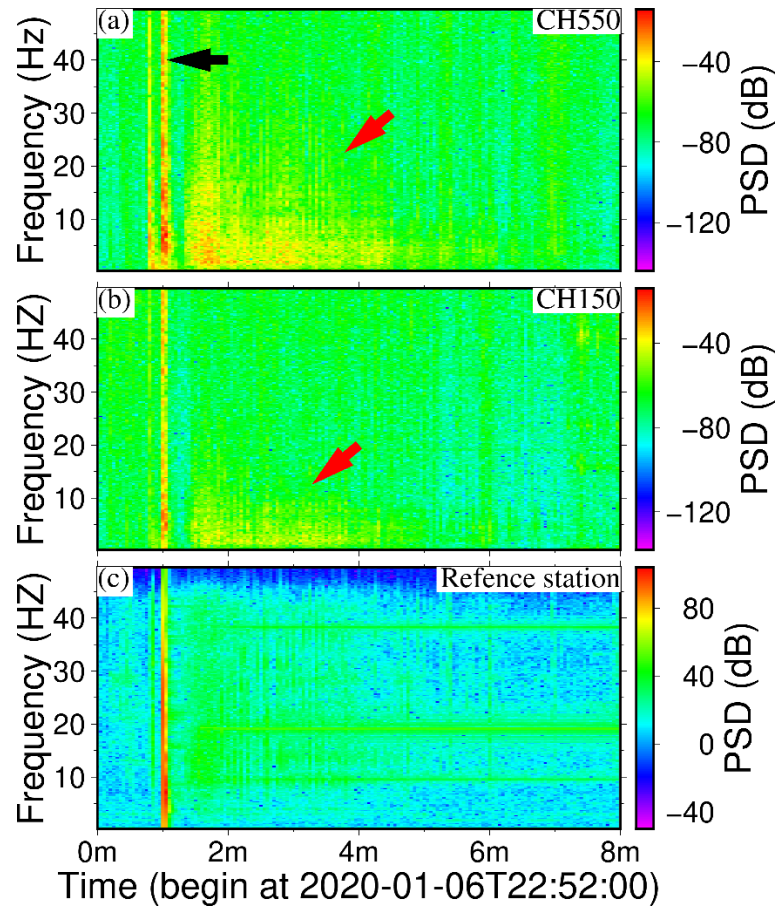
Figure S6. Spectrogram of the record around the AGE (Black arrow). (a) Channel 550 (inner circle), (b) Channel 150 (outer circle) and (c) vertical component of the reference station. Black curve marked the AGE. Red arrows indicate the LFEs.
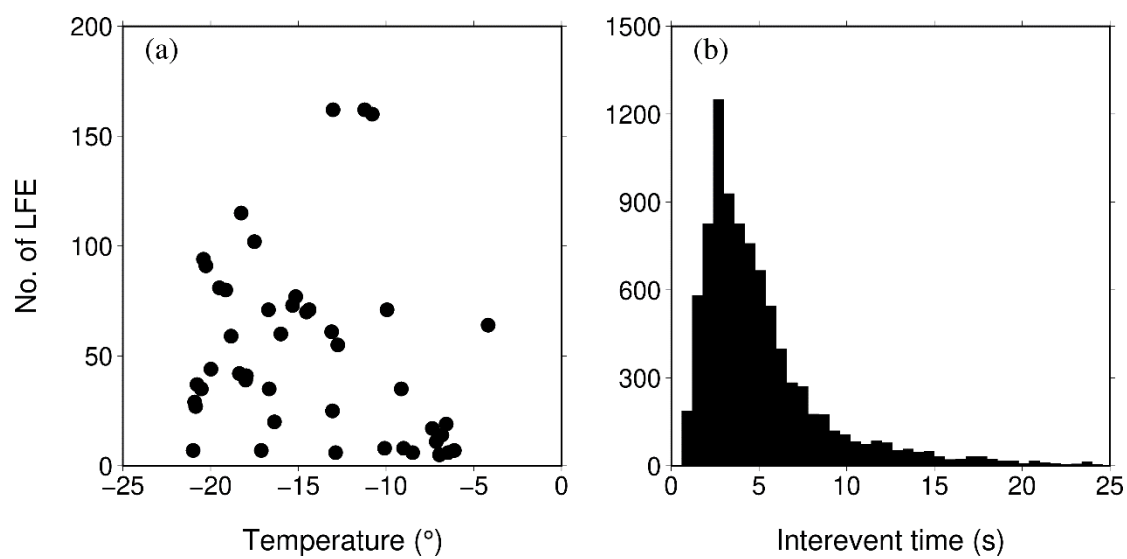
Figure S7. Statistical result of LFEs. (a) Number of LFEs versus temperature. (b) Distribution of interevent time for LFEs.
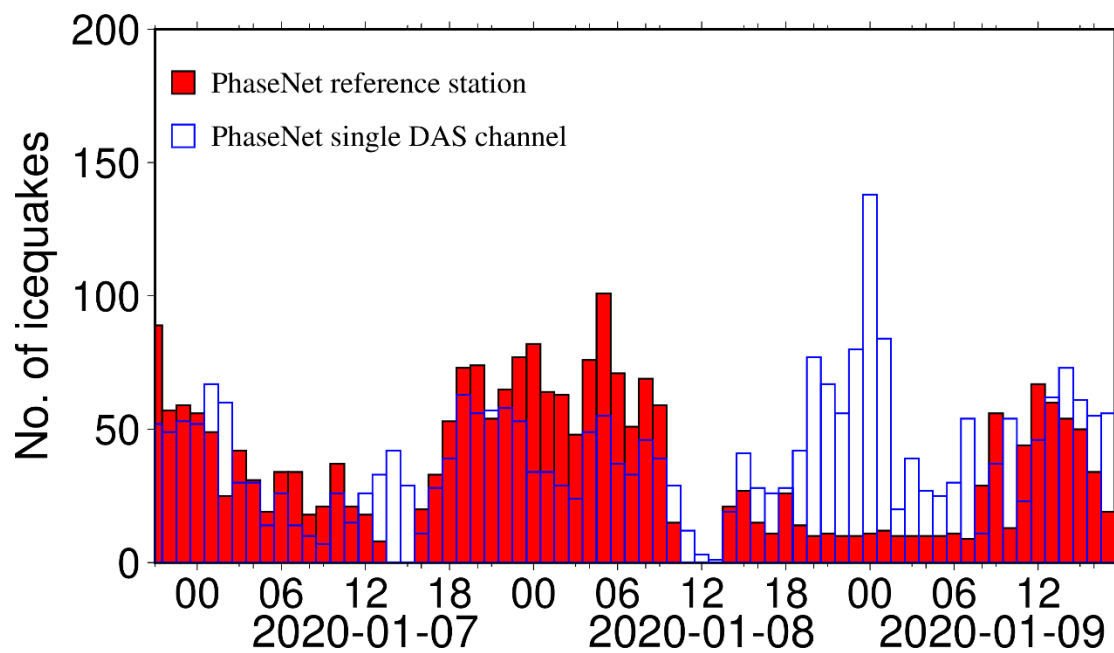
Figure S8. Number of icequakes with PhaseNet using single DAS record (blue) and reference station (red).
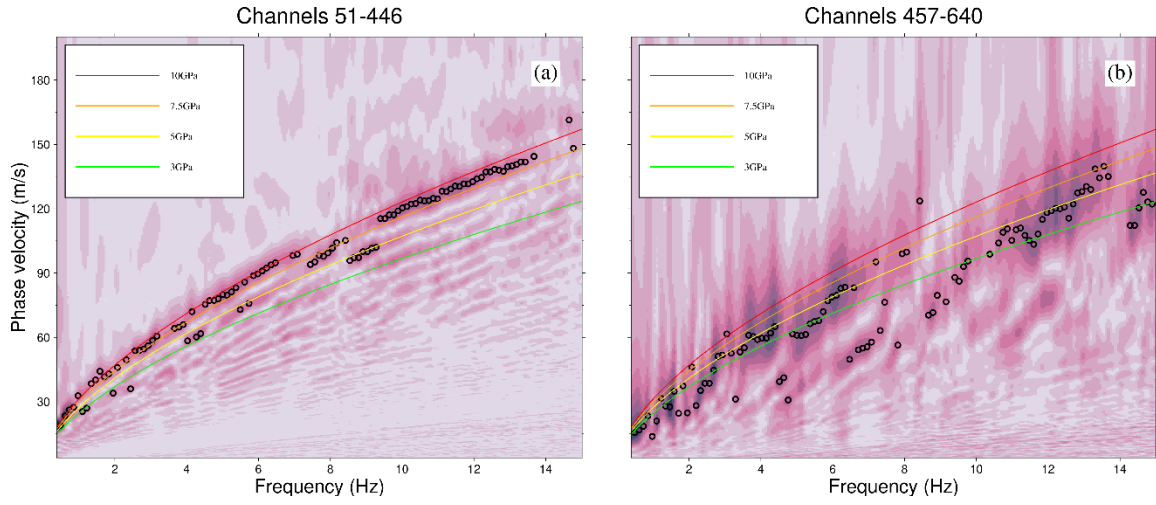
Figure S9. Dispersion curves of FGWs, the dots are the measured and the solid lines are theoretical curves with different Young's Modulus. (a) Results with DAS records of the outer circle. (b) Results with DAS records of the inner circle.
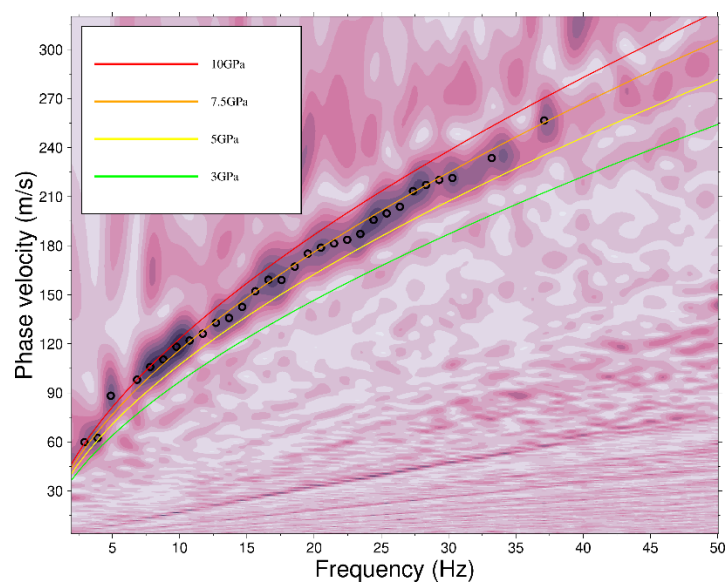
Figure S10. Dispersion curves of FGW using the signal of the red hamming point in Fig. 1.
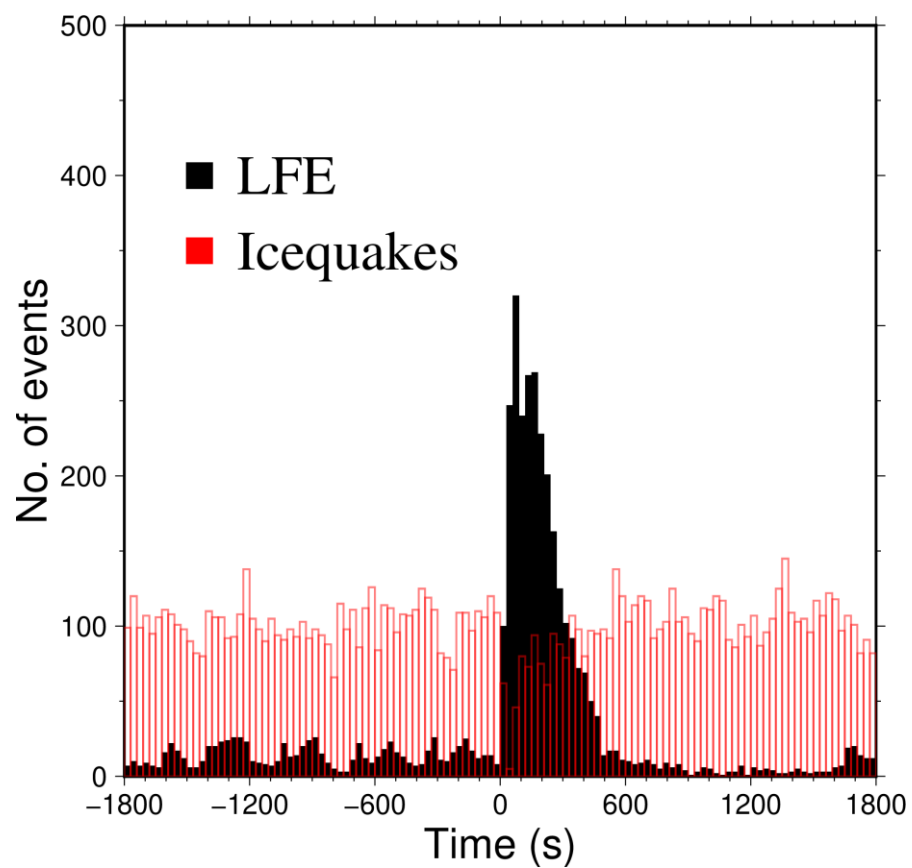
Figure S11. The number of icequakes and LFEs before and after the AGE.
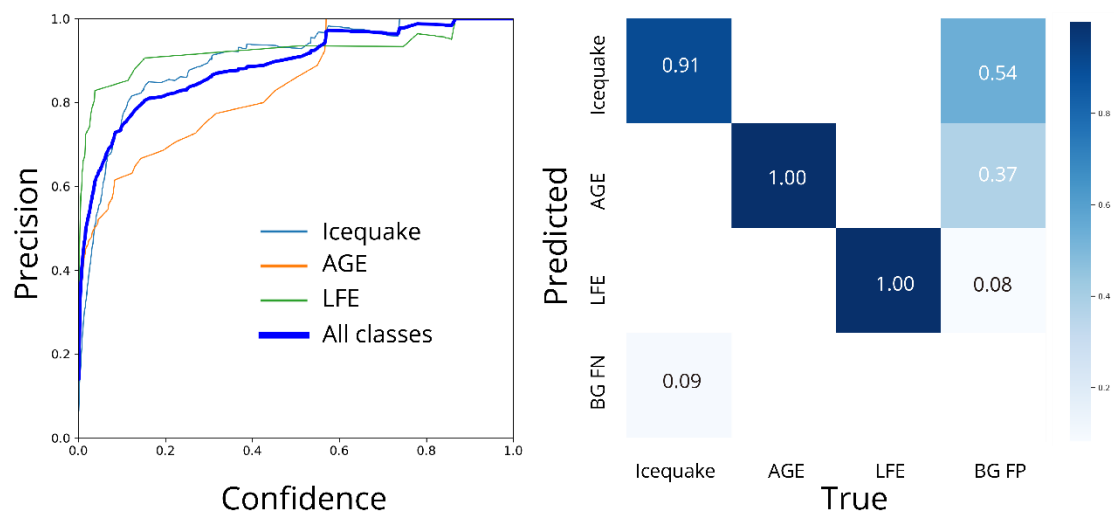
Figure S12. P curve and confusion matrix.
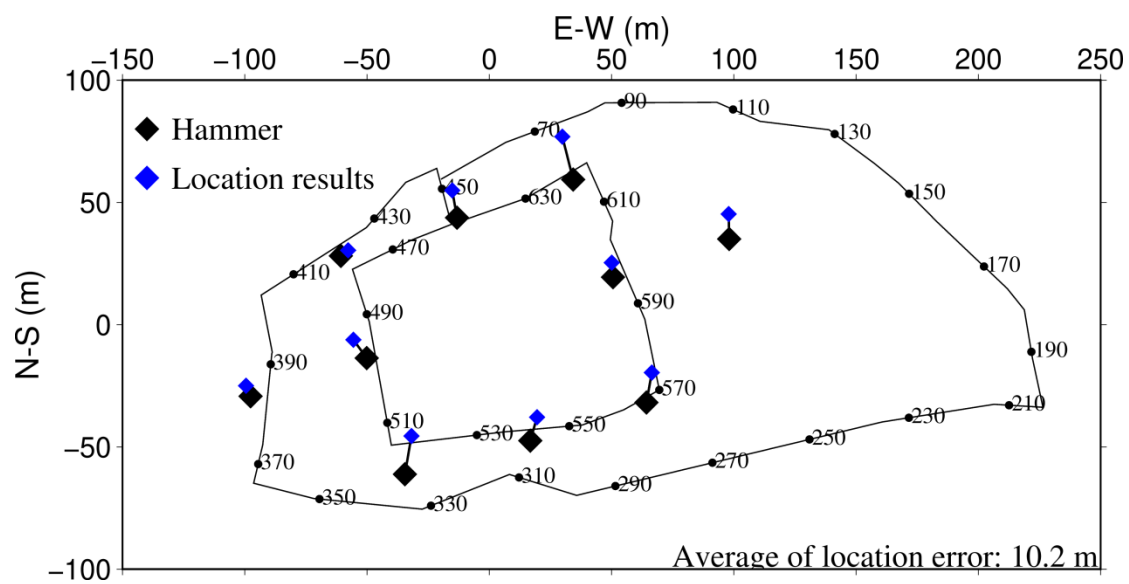
Figure S13. Hammering spots and location results.